Journal of Thermal Analysis and Calorimetry
https://doi.org/10.1007/s10973-026-15697-9

Importance of thermophysical properties of composite phase change materials in reducing lithium-ion battery temperature: a numerical and statistical approach

Uğur Moralı[1]

Received: 3 February 2026 / Accepted: 19 May 2026
© The Author(s) 2026

Abstract
Lithium-ion batteries are widely utilized in many applications where energy storage is substantial, such as electric vehicles and electrical devices. Temperature is a critical factor limiting the performance, safety, and lifespan of lithium-ion batteries, particularly under high discharge rates. Phase change materials are widely used for battery thermal management; however, their low thermal conductivity restricts their effectiveness in practical applications. In this study, an expanded graphite-enhanced RT44HC composite phase change material was applied to a lithium iron phosphate prismatic battery to investigate the influence of key thermophysical properties on thermal performance. A combined numerical–statistical approach was employed, integrating electrochemical–thermal modeling with Taguchi design and variance analysis under different operating conditions (2C–3C discharge rates and 30–35 °C ambient temperatures). The results quantitatively revealed that thermal conductivity was the dominant parameter, contributing more than 95–98% to temperature reduction across all cases. In contrast, density and specific heat capacity exhibited secondary effects, while latent heat showed negligible influence under most conditions. Moreover, the maximum contribution of thermal conductivity reached 97.91% at 35 °C and 3C discharge rate. Due to the p value of latent heat being 0.0043, there was a statistically significant relationship between the latent heat and battery temperature for only the battery thermal management system operated at 35 °C and 3C discharge rate. These findings demonstrate that heat transfer in composite phase change material systems was primarily governed by conduction rather than latent heat storage under the investigated parameter ranges. The novelty of this study lies in providing a statistically validated, quantitative ranking of thermophysical properties, offering new insights beyond the predominantly qualitative conclusions. The results contribute to the design of more effective phase change material-based battery thermal management systems by identifying the most influential parameters under realistic operating conditions.

Keywords Thermal management · Composite phase change material · Lithium iron phosphate battery · Thermal conductivity · Orthogonal design

Introduction

The continued use of fossil fuels to meet energy demand and the resulting global warming threaten life on Earth [1]. Another problem is that fossil fuel resources are limited [2]. Moreover, today the transportation sector meets its energy supply mostly from fossil fuels [3, 4]. This situation is gradually changing thanks to the developments in science, and the vehicles used in transportation contribute to overcoming many of the important problems listed above by using new energy sources [5, 6]. Secondary batteries are increasingly coming to the fore to meet transportation energy needs [7, 8]. Many companies now produce electric or hybrid vehicles and offer them to the automotive market [9]. Among the batteries used in electric vehicles, lithium-ion batteries have an advantageous position compared to other batteries [10, 11], due to their features such as high energy density [12–14], long cycle life [15, 16], and low self-discharge rates [17]. However, situations requiring rapid energy needs, such as sudden acceleration, require high discharge rates for lithium-ion batteries. While normal discharge rates such as 1C-rate cause small temperature changes in

✉ Uğur Moralı
umorali@ogu.edu.tr

[1] Department of Chemical Engineering, Eskisehir Osmangazi University, 26040 Eskisehir, Türkiye

Published online: 13 June 2026

lithium-ion batteries, lithium-ion batteries are exposed to greater temperature changes at 2C-rate and higher discharge rates, depending on the battery's chemistry, geometry, and design [11, 18, 19]. Furthermore, it is known that lithium-ion batteries show optimum performance in the temperature range of 20–40 ℃ and that lithium-ion batteries used in this temperature range have longer cycle life [20, 21]. Temperature changes in lithium-ion batteries that provide energy at room temperature and lower discharge rates will be less than those in lithium-ion batteries that provide energy at higher ambient temperatures and higher discharge rates [22–24]. When the conditions under which lithium-ion batteries provide energy become more challenging (high discharge rate and high ambient temperature), the temperature of lithium-ion batteries may rise above the recommended temperature range for optimum performance [25, 26]. This may cause lithium-ion batteries to deplete more quickly and may also lead to thermal vulnerabilities [27, 28]. High temperature variation with high energy demand is a major challenge for lithium-ion batteries [29]. To overcome this challenge, battery thermal management systems have been introduced [25, 30–34]. Battery thermal management systems play an important role in controlling the temperatures of batteries. Air cooling [35, 36], liquid cooling [37, 38], cooling with phase change material [39, 40], and hybrid cooling systems [41–43] are included in the literature. Phase change materials with high energy storage density have a significant potential to be used in passive thermal management of lithium-ion batteries [44, 45]. Although there are organic or inorganic-based phase change materials, paraffin-containing phase change materials come to the fore [46, 47]. However, the low thermal conductivity values of phase change materials limit their use in thermal management systems [48–50]. In the literature, various materials have been added to pure phase change materials to enhance their thermophysical properties, especially thermal conductivity [51, 52]. In order to enhance the cooling performance of the phase change material in the battery thermal control system, Subramanian et al. implemented a passive cooling technique using a paraffin-based phase change material to determine the optimal additive material [53]. Their research indicated that the expanded graphite was the best option of additive materials, improving the thermal conductivity of the thermal management system. Nevertheless, a higher fraction of expanded graphite in composite phase change materials yields an increase in thermal conductivity, but it reduces the heat capacity and latent heat [54]. In other words, incorporating the expanded graphite changes the thermophysical properties of the pure phase change material. Therefore, it is essential to control the concentration of expanded graphite in the composite phase change materials. Moreover, it is vital to study the relationship between thermophysical properties and expanded graphite concentration to improve the thermal control performance of composite phase change materials. However, there are limited studies in the literature examining the association between the thermophysical properties of composite phase change materials and thermal management performance based on the expanded graphite content. These limited number of studies are summarized below.

Xiang et al. investigated a cold plate and phase change material battery thermal management system for high C-rate applications [55]. To reduce paraffin leakage during phase change, composite phase change materials were prepared by impregnating graphite foam with a mixture of paraffin and encapsulated paraffin microparticles. A cold plate system was also designed to remove the heat stored in the entire system. The proposed battery thermal management system was tested at high rates of 15C–21C. By comparing two different composite phase change materials with varying latent heat values, the effect of latent heat on heat removal efficiency was determined. Their results showed that the sodium sulfate decahydrate-based composite phase change material (higher latent heat) maintained a very low liquid fraction of around 3.8% by the end of the cycles, compared to 89% observed in the octadecane-based composite phase change material (lower latent heat). This result demonstrated the superior thermal persistence and advanced operational capacity of the sodium sulfate decahydrate-based system and showed the importance of the thermophysical properties of composite phase change material. In another study, Saudi et al. prepared composite phase change materials of RT35HC by using expanded graphite with different weight percentages [56]. The temperature of the battery pack was measured over a cycle test under three different cooling scenarios: natural convection, pure RT35HC, and composite phase change material with 12 mass% expanded graphite. The maximum temperatures for natural convection, pure RT35HC, and composite phase change material were recorded as 41.5 ℃, 32.3 ℃, and 29.7 ℃, respectively. The results showed the enhanced thermal management performance of the composite phase change material. Jia et al. proposed a phase change material-coupled microchannel liquid cooling composite battery thermal management system for 18,650-type cylindrical battery modules [57]. The effect of expanded graphite concentration on the composite phase change materials was investigated. The results indicated that with increasing expanded graphite content, the thermal conductivity increased, and specific heat capacity and latent heat of phase change decreased. They also determined that increasing the mass fraction of expanded graphite decreased the battery temperature and reduced the temperature uniformity. The study showed the significant influence of thermophysical properties on the battery temperature. Li et al. synthesized a composite phase change material using biomass-derived carbon and expanded graphite to improve the thermal characteristics of paraffin wax [58]. The developed composite

phase change material exhibited a higher thermal conductivity than that of the pure phase change material. The results revealed that optimization of thermal conductivity enhancement further improved heat dissipation and phase change utilization efficiency, highlighting the critical role of composite phase change material properties. Huang et al. investigated the influence of thermophysical properties (thermal conductivity, latent heat, and porosity) on the thermal management performance of composite phase change material [59]. The results showed that better thermal performance was obtained at larger thermal conductivity and latent heat of absorption. In another study, Li et al. studied the thermal management performance of composite phase change material for a battery module and determined the relative importance of thermophysical properties on the thermal management performance [60]. The results revealed that the phase transition temperature of the composite phase change material had the strongest influence on the maximum battery temperature and temperature difference. It was also found that the influence of thermal conductivity and latent heat was lower than that of the phase transition temperature. Moreover, the results demonstrated that a 10% decline in phase transition temperature decreased the maximum battery temperature by 7.9%. Napa et al. investigated the influence of various critical phase change material properties, including thermal conductivity, latent heat, melting temperature, and thickness, on a cylindrical lithium-ion battery thermal management [61]. They determined the optimum boundary conditions of the critical parameters, providing minimum battery temperature at a 3.2 C-rate and 35 ℃ ambient temperature. The critical point for thermal conductivity was determined, and the results implied that the thermal conductivity higher than 13 W m^{-1} K^{-1} showed an insignificant influence on the thermal control performance. In a recent study, Zhang et al. performed a correlation analysis between the thermophysical properties of phase change material (thermal conductivity, specific heat capacity, melting temperature, density, and latent heat) and battery thermal management performance [62]. The results showed that there was a positive correlation between melting temperature and maximum battery temperature. Moreover, the results showed that the density was negatively associated with the specific heat, and the latent heat was inversely correlated with the thermal conductivity. It has been determined that different parameters were related to each other at different discharge rates. Therefore, it has been suggested that the thermophysical properties of phase change material need to be selected based on the operating conditions. All the studies mentioned above show how important the investigation of thermophysical features of composite phase change materials is, while showing the influences of thermophysical properties of phase change materials in reducing the temperature of the lithium-ion battery systems. Thus, the future of studies on the design of phase change materials used in battery thermal management systems is bright, and further studies are still needed on this subject. Thermophysical properties of composite phase change materials are important parameters for the optimization and design of battery thermal management systems. In order to effectively design robust thermal management systems containing composite phase change materials, the effects of these thermophysical properties on battery temperature should be investigated under various loads, such as distinct discharge rates and ambient temperatures. However, the influences of thermophysical properties on battery thermal management have not been quantitatively determined. Moreover, the relative effects of thermophysical properties such as density, specific heat capacity, thermal conductivity, and latent heat on the battery temperature have not been numerically demonstrated. Determining these effects mathematically/numerically will reveal which thermophysical properties should be given importance in the design of battery thermal management systems using composite phase change materials. Additionally, the contribution of each thermophysical property of the composite phase change material to the increase in battery temperature under various conditions has not been quantitatively determined. A holistic statistical approach that determines all these effects will be very important in the design of composite phase change materials and thermal management of lithium-ion batteries. In this context, the main novelty and contributions of this study can be summarized as follows:

- A quantitative evaluation of the relative importance of thermophysical properties (density, specific heat capacity, thermal conductivity, and latent heat) on lithium-ion battery temperature using a combined Taguchi-ANOVA framework,
- Determination of the contribution ratios of each thermophysical property under different operating conditions (varying ambient temperatures and discharge rates),
- A combined numerical and statistical approach to identify the dominant parameters affecting thermal management performance.

In this study, a battery thermal management system consisting of an RT44HC phase change material enhanced with expanded graphite was proposed. The thermophysical properties, such as density, specific heat capacity, thermal conductivity, and latent heat, were determined for the composite phase change material, including different concentrations of expanded graphite. For different discharge conditions (moderate C-rate of 2C, and moderate ambient temperature of 30 ℃ and high Crate of 3C, and high ambient temperature of 35 ℃), an orthogonal array design was utilized to numerically and statistically demonstrate the relative significance of each thermophysical property on

the thermal control performance of the composite phase change materials. The contribution of each thermophysical property associated with the expanded graphite content in the phase change material was calculated to minimize the lithium-ion battery temperature. In addition, the statistical significance of thermophysical parameters was demonstrated using ANOVA under realistic battery operating conditions. The rest of the paper is organized as follows. Section "Materials and methods" describes the numerical method, statistical analysis procedures, and limitations of the model. Section "Results and discussion" analyzes the Taguchi design of experiment results and presents variance analysis. The relative importance of thermophysical properties of composite phase change material is discussed in Sect. "Discussion," while Sect. "Limitations" presents some limitations. Finally, the study is concluded in Sect. "Conclusion."

Materials and methods

In this section, brief information about various properties of lithium-ion battery, problem definition, applied battery thermal model, phase change material model, and orthogonal array design is presented.

Lithium-ion battery

In this present work, a prismatic lithium-ion battery with a lithium iron phosphate cathode and a graphite anode was used. The nominal voltage and capacity of the battery are 3.20 V and 50 Ah, respectively. The potential window of the battery is between 3.65 V (maximum potential) and 2.50 V (minimum potential). Various specifications of the lithium-ion battery are shown in Table 1. The geometric structure and physical dimensions of the lithium-ion battery are shown in Fig. 1.

Table 1 Basic parameters of lithium-ion prismatic battery cell [63]

Parameters	Value	Unit
Nominal voltage	3.20	V
Nominal capacity	50	Ah
Energy density	130	W kg^{-1}
End voltage	2.50	V
Charging voltage	3.65	V
Anode material	Graphite	
Cathode material	$LiFePO_4$	
Electrolyte material	Carbonate-based	
Dimensions	29.3 × 135 × 180	mm

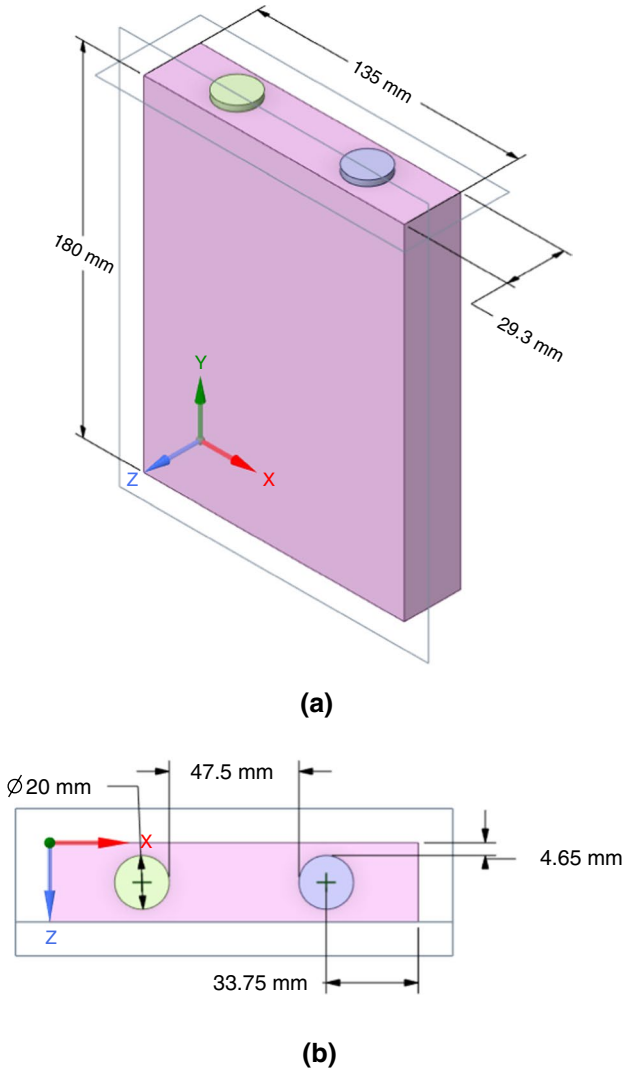


Fig. 1 Dimensions of a prismatic lithium-ion battery: **a** 3-dimensional view and **b** top view

Problem statement

Investigating the thermal behavior of lithium-ion batteries under various load conditions is crucial for the development of energy storage devices. Therefore, in this study, the thermal behavior of the prismatic lithium-ion battery at medium (35 ℃) and high (40 ℃) temperatures was investigated. The battery was discharged from 3.65 V potential to 2.50 V potential at 2C and 3C rates at these two ambient temperatures, and the battery temperature was determined numerically. A phase change material-based battery thermal management system was proposed to control the battery temperature and reduce the temperature rise during the discharge process. Moreover, a composite phase change material containing expanded graphite was designed to enhance the thermophysical properties of the phase change

material. The designed battery thermal management system is presented in Fig. 2. Adding expanded graphite to the phase change material changed the thermophysical properties of the resulting composite phase change material. The effects of the composite phase change material, whose thermophysical properties change with the incorporation of expanded graphite, on the battery temperature were determined using an orthogonal array design. The main effects of thermophysical properties (density, specific heat capacity, thermal conductivity, and latent heat) on battery temperature were determined statistically by the Taguchi experimental design method. Thus, the thermophysical property that has the most effect on preventing battery temperature increase could be determined. Moreover, the contribution of each thermophysical property to the decrease in battery temperature was demonstrated numerically.

Numerical method

Electrochemical–thermal modeling techniques are used to estimate the temperature of lithium-ion batteries. This study employs a modeling approach based on the Multi-Scale Multi-Domain (MSMD) framework, integrating the Newman, Tiedemann, Gu, and Kim (NTGK) model. It accounts for both Joule heating and heat generated from electrochemical reactions. The governing equations are solved numerically using the finite volume method within the ANSYS Fluent simulation environment. A pressure-based solver is utilized alongside a transient thermal model.

In constructing the battery model, the material is assumed to have uniform density and specific heat capacity, with thermal conductivity treated as constant throughout the domain. The numerical characteristics of the lithium-ion battery used in the simulations are presented in Table 2.

The following equation describes the energy conservation within the battery [66]:

$$\frac{\partial}{\partial t}\left(\rho c_{\mathrm{p}} T\right) = \nabla(\lambda \nabla T) + Q_{\mathrm{g}} \tag{1}$$

where t is time, ρ signifies the density of the battery material; c_{p} represents the battery's specific heat capacity; T corresponds to the temperature field within the battery; λ is the thermal conductivity; and Q_{g} quantifies the heat generation occurring internally in the battery.

Heat generation in the battery, represented by Q_{g}, comprises three fundamental contributions: the reaction heat (Q_{r}), polarization heat (Q_{p}), and Joule heat (Q_{j}), which can be mathematically formulated as follows:

$$Q_{\mathrm{g}} = Q_{\mathrm{r}} + Q_{\mathrm{p}} + Q_{\mathrm{j}} \tag{2}$$

The thermal energy produced as a result of internal chemical processes is denoted as:

$$Q_{\mathrm{r}} = -T_{\mathrm{b}} \Delta S \frac{I}{nF} \tag{3}$$

where ΔS signifies the change in entropy, I indicates the magnitude of the electric current, n corresponds to the

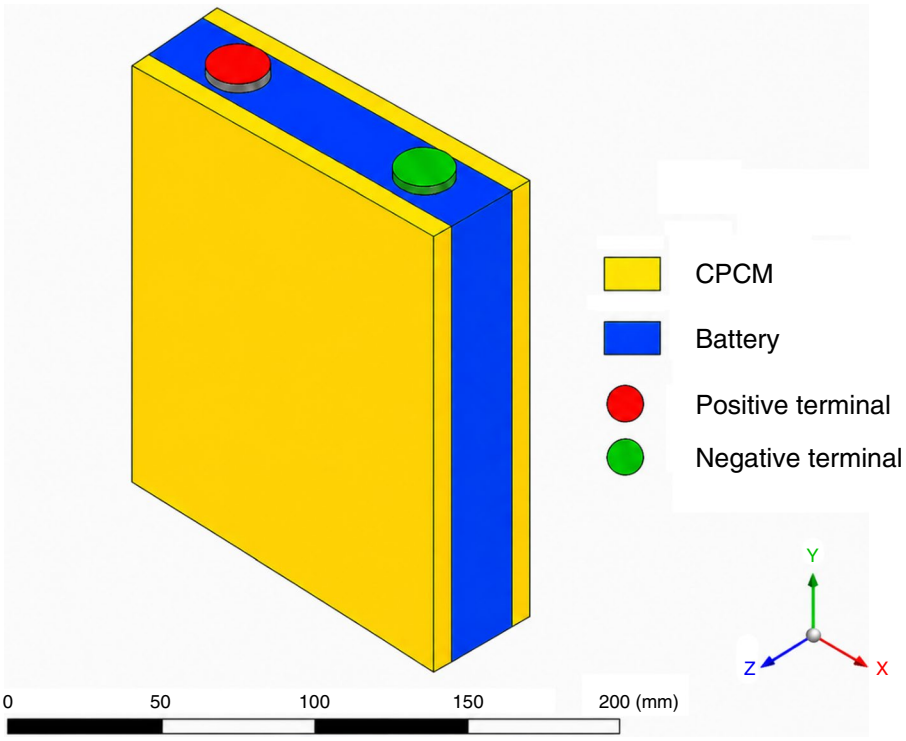


Fig. 2 Lithium-ion battery thermal management system. Both sides of the battery are surrounded by expanded graphite-based composite phase change material

Table 2 Thermophysical properties of lithium-ion battery cell

Parameters	Value	Unit	References
Density of positive tab	2719	kg m^{-3}	[63]
Density of negative tab	8978	kg m^{-3}	[63]
Density of battery	1868	kg m^{-3}	[63]
Specific heat capacity of positive tab	871	J kg^{-1} K^{-1}	[63]
Specific heat capacity of negative tab	381	J kg^{-1} K^{-1}	[63]
Specific heat capacity of battery	1296	J kg^{-1} K^{-1}	[63]
Thermal conductivity of positive tab	202.4	W m^{-1} K^{-1}	[63]
Thermal conductivity of negative tab	387.6	W m^{-1} K^{-1}	[63]
Thermal conductivity of battery	$k_x = k_y = 2.7$ $k_z = 0.9$	W m^{-1} K^{-1}	[63]
Conductance for positive tab	3.541e + 07	S m^{-1}	[63]
Conductance for negative tab	5.800e + 07	S m^{-1}	[63]
Internal resistance of battery	0.015	Ω	[64, 65]

number of electrons transferred during the electrochemical process, and F represents the Faraday constant.

Heat generated by polarization—resulting from the departure of the electrode potential from its equilibrium state—is quantified using the following equation:

$$Q_p = I^2 R_p = I^2 \left(R_t - R_e\right) \tag{4}$$

where R_p, R_t, and R_e show the resistance polarization, the total resistance, and the real resistance, respectively.

The thermal energy produced due to the resistive properties of the battery can be articulated in the following manner:

$$Q_j = I(E - V) = I^2 R_e \tag{5}$$

where E represents the voltage in an open-circuit condition, whereas V signifies the voltage during operation.

Consequently, the thermal energy generated by the battery may be encapsulated as follows:

$$Q_g = -T_b \Delta S \frac{I}{nF} + I^2 R \tag{6}$$

Mesh independence and validation of the model

One of the fundamental and critical initial steps of numerical studies is meshing, which is the division of the created geometry into small control volumes. Generally, increasing the number of mesh elements improves the accuracy of the calculation results, but it also increases the computation time. Conversely, reducing the number of mesh elements may result in decreased accuracy of results while lessening computational time. Therefore, in numerical studies, mesh independence testing is performed after the geometry/structure to be examined is created. ANSYS Fluent Meshing tools were used to produce hexahedral meshes in the present study. To balance time and accuracy, the prismatic lithium-ion battery geometry created in ANSYS Fluent Design Modeler was subdivided into hexahedral elements with dimensions ranging from 4 to 2 mm for mesh independence analysis. Lithium-ion battery temperatures obtained for various element sizes are presented in Table 3.

10,790 and 92,660 control volumes were obtained for 4 mm and 2 mm element sizes, respectively. The temperature for the 4 mm element size was 40.366 ℃, while for the 2 mm element size it was 40.431 ℃. Lithium-ion battery temperature increased with decreasing element size from 4 to 3 mm, and then an equilibrium in the lithium-ion battery temperature values was reached with further decreasing element size, as shown in Fig. 3. The lithium-ion battery temperature increased from 40.420 ℃ to 40.425 ℃ with the decrease in element size from 2.50 to 2.25 mm, and this increase was considered to be negligible. In order to establish a balance between simulation time and element number, the convenient element size was selected as 2.50 mm for further studies. The mesh structure of the lithium-ion battery with an element size of 2.50 mm is shown in Fig. 4.

Another important step of the simulation is the comparison of numerical results with experimental results. The compatibility of experimental and numerical results is important for the reliability of the results obtained from numerical studies. Therefore, in this study, after determining the appropriate mesh number in the previous step, the temperature

Table 3 Relationship between element size and lithium-ion battery temperature

Size/mm	Element number	Battery temperature/℃
4.00	10,790	40.366
3.00	27,388	40.408
2.50	47,236	40.420
2.25	63,028	40.425
2.00	92,660	40.431

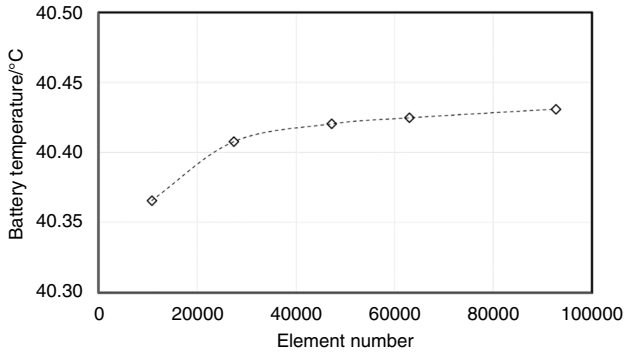


Fig. 3 Grid independence study: relationship between element number and lithium-ion battery temperature

of the lithium-ion battery discharged experimentally with different discharge rates was compared with the numerically obtained results. The lithium-ion battery was discharged from 3.65 to 2.50 V at different discharge rates (1C, 2C, and 3C) at an ambient temperature of 30 ℃. At the beginning of the discharge process, the ambient temperature and the temperature of the lithium-ion battery were equal.

In order to test the accuracy of the simulation studies performed in ANSYS Fluent, the results of the experimental studies conducted by Zhang et al. [63] in the literature were compared with the results of the numerical studies performed in this study. Figure 5 shows the variation of lithium-ion battery temperature during discharge processes, both experimentally and numerically. The results showed that the experimental and numerical results were in good agreement with each other. Moreover, the lithium-ion battery temperatures obtained at the end of the discharge periods are presented in Table 4. The results showed that the final battery temperatures obtained experimentally and numerically were very close to each other, and the difference between them was less than 1 ℃. The results of the verification showed that the mesh size selected in the previous section was appropriate, and the applied battery thermal model can be used in the subsequent sections.

Enthalpy change method for phase change material

The enthalpy change approach was utilized to investigate the thermal transport phenomena in the phase change material. The enthalpy-based energy conservation equation (general form) is expressed as follows:

$$\frac{\partial(\rho H)}{\partial t} + \nabla \cdot (\rho \mathrm{V} H) = \nabla \cdot (k \nabla T) \tag{7}$$

where, ρ is the density, H is the total enthalpy, k is the thermal conductivity, $\mathrm{V} = (u, v)$ is the velocity vector.

Continuity equation

$$\frac{\partial(\rho_{\mathrm{pcm}})}{\partial t} + \frac{\partial(\rho_{\mathrm{pcm}} u)}{\partial x} + \frac{\partial(\rho_{\mathrm{pcm}} v)}{\partial y} = 0 \tag{8}$$

where u and v are the velocity components in the x- and y-directions.

Momentum equation

$$\frac{\partial(\rho_{\mathrm{pcm}} u)}{\partial t} + \frac{\partial(\rho_{\mathrm{pcm}} u^2)}{\partial x} + \frac{\partial(\rho_{\mathrm{pcm}} uv)}{\partial y} = -\frac{\partial p}{\partial x} + \mu\left(\frac{\partial^2 u}{\partial x^2} + \frac{\partial^2 u}{\partial y^2}\right) + S \tag{9}$$

where P indicates the pressure, μ denotes the dynamic viscosity, and S denotes the momentum source term.

The source term is defined as:

$$S = -A_{\mathrm{mush}} \frac{(1-\beta^2)}{\beta^3 + \varepsilon} V \tag{10}$$

where A_{mush} is the mushy zone constant, and ϵ is a small number to prevent division by zero.

The density of the PCM is assumed to be constant, and buoyancy-driven natural convection is neglected due to the presence of expanded graphite, which forms a porous structure that significantly suppresses fluid motion within the composite.

Energy equation (PCM domain)

By applying Eq. (7) to the PCM region, the governing energy equation becomes:

$$\frac{\partial(\rho_{\mathrm{pcm}} h_{\mathrm{e}})}{\partial t} + \frac{\partial(\rho_{\mathrm{pcm}} u h_{\mathrm{e}})}{\partial x} + \frac{\partial(\rho_{\mathrm{pcm}} v h_{\mathrm{e}})}{\partial y} = \frac{\partial}{\partial x}\left(k_{\mathrm{pcm}} \frac{\partial T}{\partial x}\right) + \frac{\partial}{\partial y}\left(k_{\mathrm{pcm}} \frac{\partial T}{\partial y}\right) \tag{11}$$

Enthalpy-based energy formulation

The total enthalpy H is defined as:

$$H = h_{\mathrm{e}} + \Delta H \tag{12}$$

where h_e is the sensible enthalpy, and ΔH represents the latent heat associated with phase change.

The sensible enthalpy is expressed as:

$$h_{\mathrm{e}} = h_{\mathrm{ref}} + \int_{T_{\mathrm{ref}}}^{T} C_{\mathrm{p}} \mathrm{d}T \tag{13}$$

where h_{ref} is reference enthalpy, T_{ref} is reference temperature, and c_{p} is specific heat capacity.

And the latent heat term is given by:

$$\Delta H = \beta L \tag{14}$$

where L is the latent heat of fusion and β is the liquid fraction, which ranges from 0 (solid) to 1 (liquid), thereby capturing the phase change process in the numerical model.

The liquid fraction is defined as:

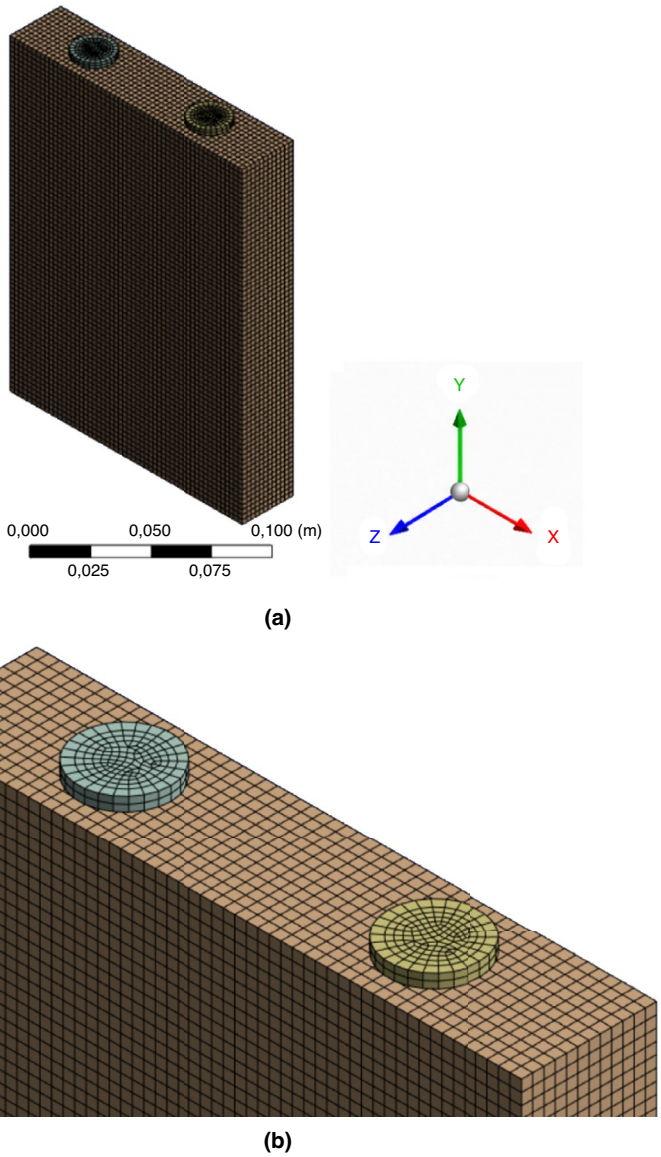


Fig. 4 Meshed model **a** prismatic lithium-ion battery, **b** a close insight into this meshing

$$\beta = \begin{cases} 0, & T < T_s \\ \frac{T-T_s}{T_l-T_s}, & T_s \le T \le T_l \\ 1, & T > T_l \end{cases} \tag{15}$$

where T_s and T_l refer to the solidus and liquidus temperatures, respectively.

Limitations of the model

The present study involves several simplifying assumptions that should be acknowledged when interpreting the results. First, buoyancy-driven natural convection within the PCM domain is not considered. The gravity term is omitted from the momentum equation, and the density of the PCM is assumed to be constant and identical in both solid and liquid phases. In addition, the inclusion of the mushy zone source term effectively suppresses fluid motion, resulting in a conduction-dominated heat transfer mechanism. While this assumption is physically reasonable for composite PCMs containing expanded graphite, where the porous structure restricts fluid mobility, it may lead to deviations under conditions where natural convection becomes non-negligible. Second, the composite PCM is assumed to remain homogeneous and structurally stable throughout the phase change process. Possible sedimentation, phase separation, or structural redistribution of expanded graphite particles is not taken into account. In practical applications, such effects may alter the effective thermophysical properties of the material and influence the thermal performance of the system. Therefore, the results presented in this study should be interpreted within the framework of a conduction-dominated and structurally stable PCM system.

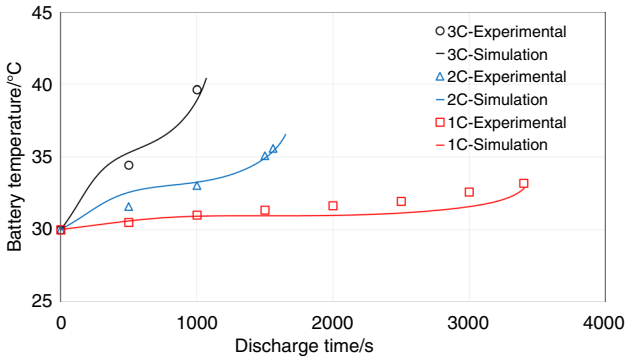


Fig. 5 Comparison of the simulation results of the current study with prior experimental data

Table 4 Experimental and numerical lithium-ion battery temperatures obtained at the end of the discharge process

Discharge rate	Battery temperature/℃	
	Simulation	Experiment
1C	32.87	33.20
2C	36.58	35.60
3C	40.42	39.65

Future studies may focus on incorporating buoyancy effects and multiphase structural evolution to further improve the accuracy and predictive capability of the model.

Initial and boundary conditions

The computational domain (Fig. 2) is subjected to the following initial and boundary conditions. At the beginning of each simulation, the entire computational domain is assumed to be at a uniform ambient temperature:

$$t = 0,\ T(x, y, z) = T_a \tag{16}$$

where T_a represents the ambient temperature, taken as 30 °C and 35 °C in this study.

The thermal interaction at the battery–phase change material interface is characterized by the following boundary condition:

$$k_b \frac{\partial T_b}{\partial n} = k_{PCM} \frac{\partial T_{pcm}}{\partial n} \tag{17}$$

where k_b and k_{pcm} are the thermal conductivities of the battery and phase change material, respectively. The thermal contact resistance between the battery cell and the composite phase change material was neglected. This assumption may slightly overestimate heat transfer; however, it allows for a clearer evaluation of the intrinsic thermophysical effects of the composite phase change material.

At the external surfaces, convective heat transfer between the system and the ambient air is modeled using Newton's law of cooling:

$$-k_{pcm} \frac{\partial T}{\partial n} = h\left(T_S - T_a\right) \tag{18}$$

where T_s is its surface temperature. The natural convective heat transfer coefficient (h) is taken as an external convective boundary condition. In this study, a constant convective heat transfer coefficient of $h = 5$ W m^{-2} K^{-1} is applied.

Orthogonal array design

Orthogonal arrays are used in the Taguchi experimental design. Orthogonal arrays, known as Greco–Latin squares, provide a robust determination of the relationship between a response variable and factors. In this study, the relationship between battery temperature (response variable) and thermophysical properties of the composite phase change material (factors) was investigated. RT44HC was selected as the pure phase change material. To enhance the thermophysical characteristics of this phase change material, composite phase change materials were obtained by adding expanded graphite at different concentrations. Various thermophysical features of the composite phase change material, such as density, specific heat, thermal conductivity, and latent heat, were determined as the expanded graphite content varied. The relationship between expanded graphite content and thermophysical properties of composite phase change materials is presented in Table 5.

Within the scope of the Taguchi experimental design applied in this study, the thermophysical properties of composite phase change materials were considered as a factor. Each thermophysical property had four levels in terms of the Taguchi orthogonal design. In other words, a design with four levels of four factors was proposed. The orthogonal array of the four-factor, four-level design is presented in Table 6. Each row in the orthogonal array represents the simulation conditions. Temperature values of the lithium-ion battery were obtained by performing simulations under sixteen different conditions. Lithium-ion battery temperature was examined as the response variable, and the examined factors were aimed at minimizing this temperature value. The effect of each thermophysical property (factor) of the composite phase change material on reducing the lithium-ion battery temperature (response variable) was statistically determined at different ambient temperatures (30 ℃ and 35 ℃) and different discharge rates (2C and 3C). Each C-rate condition was simulated independently using a transient numerical model with identical initial conditions.

Table 5 Thermophysical properties of pure RT44HC, expanded graphite, and composite phase change materials used in the present study [24, 67, 68]

Level	EG mass%	Density kg m^{-3}	Specific heat capacity J kg^{-1} K^{-1}	Thermal conductivity W m^{-1} K^{-1}	Latent heat kJ kg^{-1}
RT44HC (pure)	0	800	2000	0.20	275.0
Expanded graphite	100	230	800	45	–
Level 1	3	825	1963	0.58	266.8
Level 2	6	832	1926	1.23	258.3
Level 3	9	845	1889	3.50	250.2
Level 4	12	897	1852	5.74	242.0

Table 6 Orthogonal array design of L16(4^4). 1, 2, 3, and 4 indicate the levels for each factor

Run	Density	Specific heat capacity	Thermal conductivity	Latent heat
Sim1	1	1	1	1
Sim2	1	2	2	2
Sim3	1	3	3	3
Sim4	1	4	4	4
Sim5	2	1	2	3
Sim6	2	2	1	4
Sim7	2	3	4	1
Sim8	2	4	3	2
Sim9	3	1	3	4
Sim10	3	2	4	3
Sim11	3	3	1	2
Sim12	3	4	2	1
Sim13	4	1	4	2
Sim14	4	2	3	1
Sim15	4	3	2	4
Sim16	4	4	1	3

Statistical significance based on variance analysis

Variance analysis (ANOVA) was performed according to the significance level of 95% to determine whether there was a statistically significant relationship between the factors and the response variable. The probability value (p value) was used as an indicator that represents the evidence against the null hypothesis. There is a statistically significant association between the response variable and the factor if the p value is less than a significance level of 0.05.

Results and discussion

In this section, the influences of thermophysical properties (density, specific heat, thermal conductivity, and latent heat) of composite phase change materials of RT44HC on the temperature of the lithium iron phosphate prismatic battery are presented numerically and statistically.

The Taguchi design of experiment

For thermal management of the lithium-ion battery, the expanded graphite was incorporated into RT44HC phase change material at various ratios, yielding composite phase change materials with distinct thermophysical properties. The addition of expanded graphite changed the thermophysical features of the phase change material, and the effects of these changes on the lithium-ion battery temperature were determined using the orthogonal design for each thermophysical property. Thus, the effect of each thermophysical property on reducing the lithium-ion battery temperature was statistically and numerically determined. The orthogonal array containing the thermophysical properties of the composite phase change materials is presented in Table 7. The simulation conditions presented in Table 7 were applied to lithium-ion batteries discharged at different ambient temperatures (30 ℃ and 35 ℃) and different discharge rates (2C and 3C), and the temperature values reached as a result of the discharge process were recorded for the prismatic lithium-ion battery. The temperature values of the lithium-ion battery at the end of the discharge process, discharged under distinct loads (different ambient temperatures (30 ℃ and 35 ℃) and different discharge rates (2C-rate and 3C-rate)), are presented in Table 8. The results showed that the battery thermal management system containing composite phase change material with different thermophysical properties influenced the temperature of the lithium-ion battery. When all results in Fig. 6 were analyzed, it was determined that the lowest lithium-ion battery temperature values were obtained for simulation 13 (36.27 ℃ at 30 ℃_2C, 39.86 ℃ at 30 ℃_3C, 40.93 ℃ at 35 ℃_2C, and 44.09 ℃ at 35 ℃_3C). It was seen that the composite phase change material providing the lowest lithium-ion battery temperature had a density of 897 kg m^{-3}, a specific heat capacity of 1963 J kg^{-1} K^{-1}, a thermal conductivity of 5.74 W m^{-1} K^{-1}, and a latent heat of 258.3 kJ kg^{-1}. When the results were evaluated together with the thermophysical properties in Table 5, it was seen that such a composite phase change material had high density, low specific heat capacity, high thermal conductivity, and moderate latent heat.

Table 7 Orthogonal array design of L16. The evaluated factors that can influence the lithium-ion battery temperature were density, specific heat capacity, thermal conductivity, and latent heat. Each row shows the thermophysical properties of the composite phase change material used in the simulations

Run	Density kg m^{-3}	Specific heat capacity J kg^{-1} K^{-1}	Thermal conductivity W m^{-1} K^{-1}	Latent heat kJ kg^{-1}
Sim1	825	1963	0.58	266.8
Sim2	825	1926	1.23	258.3
Sim3	825	1889	3.50	250.2
Sim4	825	1852	5.74	242.0
Sim5	832	1963	1.23	250.2
Sim6	832	1926	0.58	242.0
Sim7	832	1889	5.74	266.8
Sim8	832	1852	3.50	258.3
Sim9	845	1963	3.50	242.0
Sim10	845	1926	5.74	250.2
Sim11	845	1889	0.58	258.3
Sim12	845	1852	1.23	266.8
Sim13	897	1963	5.74	258.3
Sim14	897	1926	3.50	266.8
Sim15	897	1889	1.23	242.0
Sim16	897	1852	0.58	250.2

Table 8 Lithium-ion battery temperatures obtained at the end of the discharge process under different loads (ambient temperatures (30 ℃ and 35 ℃) and discharge rates (2C and 3C)). The signal-to-noise ratios calculated based on the lowest-best quality characteristic of the Taguchi design, providing the creation of response tables

Run	Battery temperature/℃				Signal-to-noise ratios, S/N			
	30 ℃_2C	30 ℃_3C	35 ℃_2C	35 ℃_3C	30 ℃_2C	30 ℃_3C	35 ℃_2C	35 ℃_3C
Sim1	37.04	40.88	41.67	44.92	− 31.37	− 32.23	− 32.40	− 33.05
Sim2	36.60	40.29	41.26	44.44	− 31.27	− 32.10	− 32.31	− 32.96
Sim3	36.32	39.92	41.00	44.15	− 31.20	− 32.02	− 32.26	− 32.90
Sim4	36.29	39.91	40.98	44.10	− 31.20	− 32.02	− 32.25	− 32.89
Sim5	36.60	40.28	41.25	44.44	− 31.27	− 32.10	− 32.31	− 32.96
Sim6	37.04	40.89	41.67	44.92	− 31.37	− 32.23	− 32.40	− 33.05
Sim7	36.29	39.90	40.97	44.10	− 31.20	− 32.02	− 32.25	− 32.89
Sim8	36.32	39.93	41.00	44.15	− 31.20	− 32.03	− 32.26	− 32.90
Sim9	36.31	39.91	40.99	44.14	− 31.20	− 32.02	− 32.25	− 32.90
Sim10	36.28	39.89	40.97	44.10	− 31.19	− 32.02	− 32.25	− 32.89
Sim11	37.04	40.89	41.67	44.92	− 31.37	− 32.23	− 32.40	− 33.05
Sim12	36.60	40.29	41.26	44.44	− 31.27	− 32.10	− 32.31	− 32.96
Sim13	36.27	39.86	40.93	44.09	− 31.19	− 32.01	− 32.24	− 32.89
Sim14	36.30	39.89	40.98	44.13	− 31.20	− 32.02	− 32.25	− 32.90
Sim15	36.59	40.27	41.25	44.43	− 31.27	− 32.10	− 32.31	− 32.95
Sim16	37.03	40.88	41.67	44.92	− 31.37	− 32.23	− 32.40	− 33.05

Although the thermophysical properties of the composite phase change material that provides the lowest lithium-ion battery temperature have been determined, it is still difficult to determine which thermophysical property is effective in reducing the lithium-ion battery temperature. For this purpose, the signal-to-noise ratios in Table 8 were calculated, taking into account the lowest-best quality characteristic of the Taguchi design. The calculated signal-to-noise ratios were used to design response tables. A response table consists of the signal-to-noise ratio, delta, rank, and contribution values for each level of each factor. The signal-to-noise ratios are used to calculate the delta value of each factor, and the delta represents the importance of each factor. A factor with the highest delta value indicates that this factor is the most influential parameter on the response variable.

To determine the effect of each thermophysical property of the composite phase change materials on reducing the lithium-ion battery temperature, the response table of 30 ℃_2C-ratio was generated using the signal-to-noise ratios presented in Table 8. The response table of the lithium-ion battery temperature obtained for the battery discharged at an ambient temperature of 30 ℃ and a 2C-rate is presented in

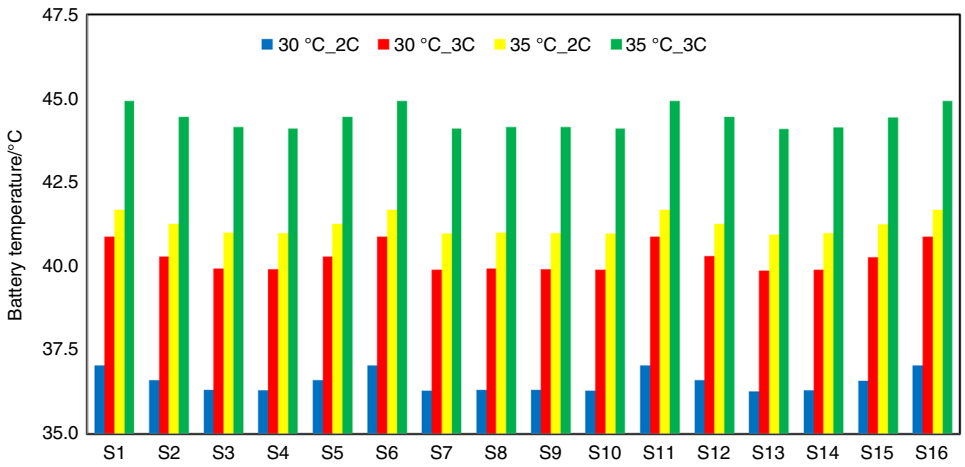


Fig. 6 Relationship between the lithium-ion battery temperature and simulation conditions. Each simulation condition represents the composite phase change material with distinct thermophysical properties

Table 9. According to Table 9, the highest delta value was obtained for the thermal conductivity, and it was 0.17837, demonstrating the highest influence of the thermal conductivity on reducing the lithium-ion battery temperature. The results showed that the density exhibited a delta value of 0.00368, indicating that its influence on reducing the lithium-ion battery temperature was the second one (lower than the thermal conductivity). Moreover, the results revealed that the delta value was 0.00255 and 0.00006 for the specific heat capacity and the latent heat, respectively. These results, presented in Table 9, revealed that the influence of the specific heat capacity on the temperature of the lithium-ion battery was greater than that of the latent heat. Thus, the relative effects of the thermophysical features of the composite phase change materials on the temperature of the lithium-ion battery were statistically determined for the lithium-ion battery discharged at an ambient temperature of 30 ℃ and a 2C-rate.

The response table of the lithium-ion battery temperature obtained for the battery discharged at an ambient temperature of 30 ℃ and a 3C-rate is presented in Table 10. The relative importance of each thermophysical property of the composite phase change material was determined based on the delta values presented in Table 10. The highest delta value was calculated for thermal conductivity with 0.21408, indicating that this value has the greatest effect in reducing the temperature of the lithium-ion battery. The density and the specific heat capacity were the second and the third influential thermophysical properties, respectively. The results showed that the latent heat with the lowest delta value of 0.00012 had the lowest impact on reducing the lithium-ion battery temperature.

The response table of the lithium-ion battery temperature obtained for the battery discharged at a surrounding air temperature of 35 ℃ and a 2C-rate is presented in Table 11. By analyzing the delta values in Table 11, it was determined that increasing the ambient temperature from 30 ℃ to 35 ℃ did not change the relative importance of each thermophysical property of the composite phase change materials. The findings revealed that the influence of the thermal conductivity on reducing the lithium-ion battery temperature was the highest, followed by the effect of the density. Similarly, it was found that the influence of the specific heat capacity was smaller than that of the density and larger than that of the latent heat. The smallest delta value of 0.00103 was calculated for the latent heat, indicating the lowest impact of the latent heat of the composite phase change material on reducing the temperature of the lithium-ion battery.

The response table of the lithium-ion battery temperature obtained for the battery discharged at an ambient temperature of 35 ℃ and a 3C-rate is presented in Table 12. The results from the response table of Table 12 showed that

Table 9 Response table of the lithium-ion battery temperature obtained for the battery discharged at an ambient temperature of 30 ℃ and a 2C-rate

Level	Density	Specific heat capacity	Thermal conductivity	Latent heat
1	− 31.260212	− 31.257667	− 31.372253	− 31.2589411
2	− 31.259852	− 31.258514	− 31.268936	− 31.2589030
3	− 31.259170	− 31.259375	− 31.200702	− 31.2589626
4	− 31.256536	− 31.260213	− 31.193879	− 31.2589632
Delta	0.00368	0.00255	0.17837	0.00006
Rank	2	3	1	4
Contribution	1.99	1.38	96.60	0.03

increasing both the ambient temperature and the discharge rate did not change the relative effects of the thermophysical properties. The results showed that, concerning the reduction in the lithium-ion battery temperature, the thermal conductivity was the most important parameter, while the latent heat was the least important factor. The density, with its delta value of 0.00193, was found to be the second influential property on the temperature of the lithium-ion battery. The results showed that the influence of the specific heat capacity was between the influences of the density and the latent heat.

In addition to determining which thermophysical property was relatively important, the contribution of each thermophysical property to reducing the temperature of the lithium-ion battery was numerically demonstrated. The contribution of each thermophysical property to the reduction in the temperature of the lithium-ion battery is presented in Table 13 and Fig. 7. For all conditions (ambient temperature and discharge rate), the thermal conductivity of the composite phase change materials made the largest contribution to reducing the lithium-ion battery temperature. This contribution was calculated as 96.60% at 30 ℃ ambient temperature and 2C discharge rate. At 30 ℃ ambient temperature, the contribution of the thermal conductivity was decreased to 95.71% with increasing the discharge rate from 2 to 3C. On the other hand, at a 2C discharge rate, the contribution of the thermal conductivity was decreased from 96.60 to 94.66% with increasing the ambient temperature from 30 ℃ to 35 ℃. Contrary, the contribution of the thermal conductivity at a 3C discharge rate increased from 95.71 to 97.91% with increasing the ambient temperature from 30 ℃ to 35 ℃. At 35 ℃ ambient temperature, the contribution of the thermal conductivity was increased from 94.66% to 97.91% with increasing the discharge rate from 2 to 3C. In other words, the highest contribution value of the thermal conductivity, as the most influential factor in reducing the temperature of the lithium-ion battery, was obtained at an ambient temperature of 35 ℃ and a discharge rate of 3C.

Although the contribution of thermophysical properties, except thermal conductivity, seems to be negligible, it is

Table 10 Response table of the lithium-ion battery temperature obtained for the battery discharged at an ambient temperature of 30 ℃ and a 3C-rate

Level	Density	Specific heat capacity	Thermal conductivity	Latent heat
1	− 32.095065	− 32.091186	− 32.231027	− 32.093127
2	− 32.094518	− 32.092475	− 32.102416	− 32.093058
3	− 32.093471	− 32.093799	− 32.022142	− 32.093170
4	− 32.089475	− 32.095069	− 32.016944	− 32.093174
Delta	0.00559	0.00388	0.21408	0.00012
Rank	2	3	1	4
Contribution	2.50	1.74	95.71	0.05

Table 11 Response table of the lithium-ion battery temperature obtained for the battery discharged at an ambient temperature of 35 ℃ and a 2C-rate

Level	Density	Specific heat capacity	Thermal conductivity	Latent heat
1	− 32.303556	− 32.300366	− 32.396858	− 32.3024573
2	− 32.303242	− 32.302087	− 32.309184	− 32.3014379
3	− 32.302656	− 32.302830	− 32.254857	− 32.3024723
4	− 32.299385	− 32.303556	− 32.247940	− 32.3024719
Delta	0.00417	0.00319	0.14892	0.00103
Rank	2	3	1	4
Contribution	2.65	2.03	94.66	0.66

Table 12 Response table of the lithium-ion battery temperature obtained for the battery discharged at an ambient temperature of 35 ℃ and a 3C-rate

Level	Density	Specific heat capacity	Thermal conductivity	Latent heat
1	− 32.947993	− 32.946730	− 33.049053	− 32.947184
2	− 32.947874	− 32.947179	− 32.955322	− 32.947271
3	− 32.947422	− 32.947527	− 32.896960	− 32.947390
4	− 32.946060	− 32.947914	− 32.888015	− 32.947504
Delta	0.00193	0.00118	0.16104	0.00032
Rank	2	3	1	4
Contribution	1.18	0.72	97.91	0.19

Table 13 Contribution of each thermophysical property of the composite phase change material in reducing the lithium-ion battery temperature. The temperature of the lithium-ion battery was obtained at the end of the discharge process under distinct loads

Condition	Contribution/%			
	Density	Specific heat capacity	Thermal conductivity	Latent heat
30℃_2C	1.99	1.38	96.60	0.03
30℃_3C	2.50	1.74	95.71	0.05
35℃_2C	2.65	2.03	94.66	0.66
35℃_3C	1.18	0.72	97.91	0.19

important to evaluate the contribution of these properties to lowering the temperature of the lithium-ion battery in order to design a robust thermal management system. The contribution of the density to lowering the temperature of the lithium-ion battery discharged at 30 ℃ and 2C-rate was 1.99%. At 30 ℃, the contribution of the density increased to 2.50% for the lithium-ion battery discharged at a 3C-rate. The highest contribution of the density was calculated for the lithium-ion battery discharged at 35 ℃ and 3C-rate. At 35 ℃, the contribution of the density decreased to 1.18% for the lithium-ion battery discharged at a 3C-rate. This contribution was the lowest value for the density. Since the contribution of the density was greatest at 35 ℃ and 2C-rate, the density value of the composite phase change materials should be carefully adjusted under these conditions.

Similarly, the contribution of the specific heat was highest with the contribution value of 2.03% for lowering the temperature of the lithium-ion battery at 35 ℃ and 2C-rate. At 30 ℃, the contributions of the specific heat were 1.38% and 1.74% at 2C-rate and 3C-rate, respectively. The lowest contribution of the specific heat was 0.72% obtained for the battery thermal management system at 35 ℃ and 3C-ratio. Since this lowest contribution of the specific heat at 35 ℃ and 3C-ratio was less than 1%, the influence of the specific heat on reducing the battery temperature at 35 ℃ and 3C-ratio can be neglected. In other words, at 35 ℃ and 3C-ratio, the density of the composite phase change material did not show a substantial influence in reducing the temperature of the lithium-ion battery.

When the contributions of the thermophysical properties of the composite phase change materials were analyzed, the latent heat exhibited the lowest impact for lowering the temperature of the lithium-ion battery. The contribution values of the latent heat were lower than 1%, indicating the negligible effect of the latent heat on the lithium-ion battery thermal management system. The highest contribution of the latent heat was observed at 35 ℃ and 3C-rate, and it was 0.66%. Moreover, the lowest contribution of the latent heat was calculated for the lithium-ion battery thermal management system at 30 ℃ and 2C-rate. At 30 ℃, the contribution of the latent heat showed a negligible increase as the discharge rate increased from a 2C rate to a 3C rate. On the other hand, at 35 ℃, the contribution of the latent heat decreased from 0.66% to 0.19% with increasing the discharge rate from 2C-rate to 3C-rate, respectively.

Summing up, the contribution of the thermal conductivity was the greatest compared to the other thermophysical properties of the composite phase change materials, showcasing the most influential effect on lowering the temperature of the lithium-ion battery. On the other hand, the latent heat exhibited the lowest influence on lowering the temperature of the lithium-ion battery, statistically demonstrated by the lowest contribution values of the latent heat. Therefore, the thermal conductivity should be carefully observed and controlled during the preparation of composite phase change materials in order to design a robust lithium-ion battery thermal management system.

Analysis of variance

Table 14 shows the statistical significance of the thermophysical properties of composite phase change materials for batteries discharged at 30 ℃ and a 2C-rate. ANOVA results presented in Table 14 revealed that thermal conductivity was the most significant parameter affecting the battery temperature ($p = 0.0000$), with a substantially larger F value compared to other thermophysical properties. Density and specific heat capacity were also found to be statistically significant ($p < 0.05$), although their contributions were relatively smaller. In contrast, latent heat did not have a statistically significant effect on battery temperature within the parameter range studied ($p = 0.4968$).

Table 15 shows the statistical significance of the thermophysical properties of composite phase change materials for batteries discharged at 30 ℃ and a 3C-rate. ANOVA results presented in Table 15 indicated that thermal conductivity remained the dominant parameter ($p = 0.0000$), while density and specific heat capacity also have statistically significant effects. Although latent heat was not statistically significant within the investigated range ($p > 0.05$), this did not imply that phase change effects were negligible; rather, it suggested that the selected variation range of latent heat was insufficient to produce a measurable impact on the lithium-ion battery temperature.

Table 16 shows the statistical significance of the thermophysical properties of composite phase change materials for batteries discharged at 35 ℃ and a 2C-rate. ANOVA results presented in Table 16 indicated that the thermal conductivity was overwhelmingly the dominant contributor to the variation in the battery temperature, accounting for nearly all of the explained sum of squares and yielding an extremely large F value, which confirmed its

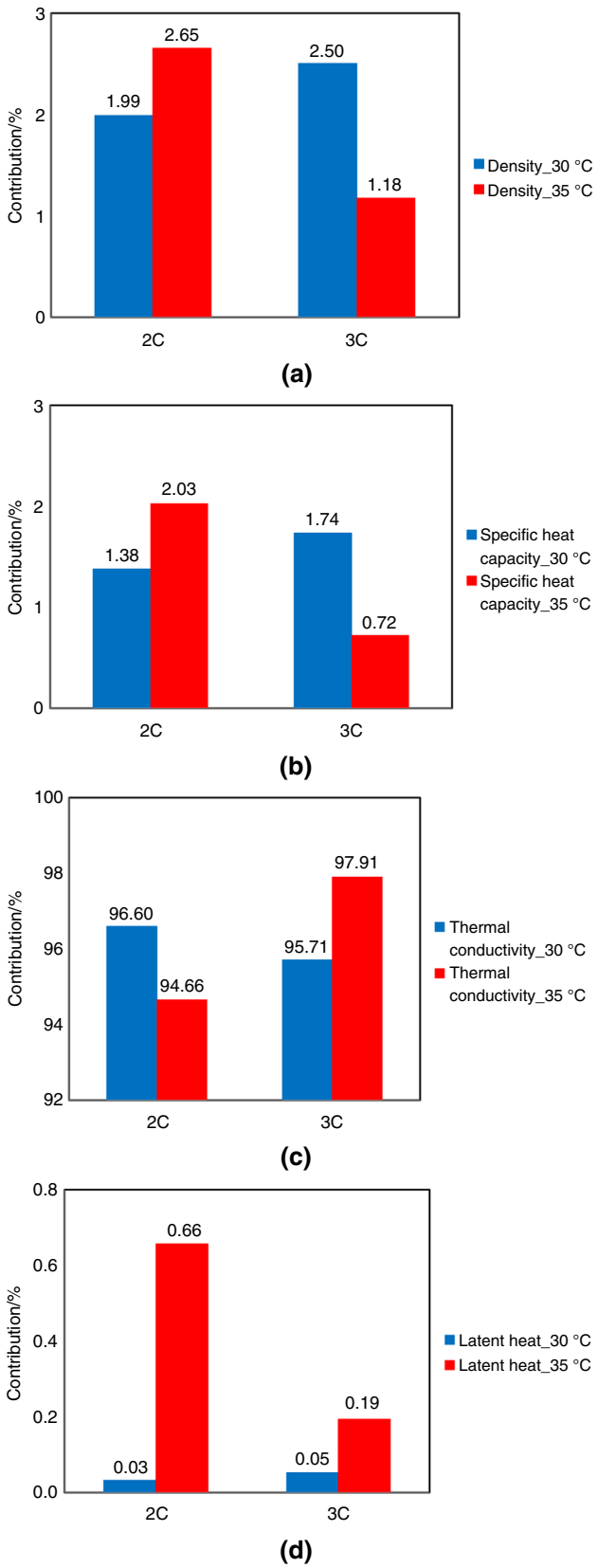


Fig. 7 Contribution of the thermophysical properties in reducing the lithium-ion battery temperature at ambient temperatures of 30 ℃ and 35 ℃ and discharge rates of 2C and 3C: **a** density, **b** specific heat, **c** thermal conductivity, and **d** latent heat

strong statistical significance. In contrast, the specific heat capacity showed statistically significant but comparatively minor effects, suggesting that it played a secondary role in fine-tuning the battery temperature rather than driving its overall behavior. On the other hand, the specific heat capacity and latent heat were not statistically significant, as reflected by their low F value and high p value.

Table 17 shows the statistical significance of the thermophysical properties of composite phase change materials for batteries discharged at 35 ℃ and a 3C-rate. ANOVA results presented in Table 17 revealed that all thermophysical properties, including latent heat, were statistically significant within the investigated parameter range. In other words, there was a statistically significant relationship between the thermophysical properties of composite phase change materials and battery temperature. Similar to other results, the thermal conductivity parameter had the strongest influence on the battery temperature compared to other thermophysical properties due to the largest F value. However, at the most demanding condition (35 °C and 3C), latent heat was statistically significant ($p = 0.0043$), indicating that its influence increased under more severe thermal loads. Despite this, its overall contribution remained considerably smaller than that of thermal conductivity.

These findings confirmed that the dominance of thermal conductivity was robust and consistent across different environmental temperatures and discharge rates. The agreement between the ANOVA results and the Taguchi analysis further validated the reliability of the conclusions. Overall, the results demonstrated that enhancing the thermal conductivity of the composite PCM was the most effective strategy for improving battery thermal management performance, while the effects of other thermophysical parameters remained comparatively limited within the investigated parameter ranges.

Discussion

The thermal performance of the battery system was evaluated under various combinations of thermophysical properties using a Taguchi-based numerical framework coupled with electrochemical–thermal simulations. The results clearly demonstrated that the thermophysical properties of the composite phase change material exhibited

Table 14 ANOVA results for the battery temperature obtained at 30 ℃ and a 2C-rate

Source	DF	Sum of squares	Mean square	*F* value	*p* value
Density	3	0.0005825	0.000194	4954.60	0.0000
Specific heat capacity	3	0.0002517	0.000084	2141.37	0.0000
Thermal conductivity	3	1.4650372	0.488346	12,462,100.16	0.0000
Latent heat	3	0.0000001	0.000000	1.01	0.4968
Error	3	0.0000001	0.000000		
Total	15	1.4658716			

Table 15 ANOVA results for the battery temperature obtained at 30 ℃ and a 3C-rate

Source	DF	Sum of squares	Mean square	*F* value	*p* value
Density	3	0.0016285	0.000543	3039.70	0.0000
Specific heat capacity	3	0.0007080	0.000236	1321.55	0.0000
Thermal conductivity	3	2.5890517	0.863017	4,832,682.69	0.0000
Latent heat	3	0.0000005	0.000000	1.01	0.4970
Error	3	0.0000005	0.000000		
Total	15	2.5913893			

Table 16 ANOVA results for the battery temperature obtained at 35 ℃ and a 2C-rate

Source	DF	Sum of squares	Mean square	*F* value	*p* value
Density	3	0.0009883	0.000329	14.08	0.0284
Specific heat capacity	3	0.0004990	0.000166	7.11	0.0710
Thermal conductivity	3	1.2847877	0.428263	18,298.17	0.0000
Latent heat	3	0.0000699	0.000023	1.00	0.5000
Error	3	0.0000702	0.000023		
Total	15	1.2864152			

Table 17 ANOVA results for the battery temperature obtained at 35 ℃ and a 3C-rate

Source	DF	Sum of squares	Mean square	*F* value	*p* value
Density	3	0.0002447	0.000082	2145.68	0.0000
Specific heat capacity	3	0.0000783	0.000026	686.09	0.0000
Thermal conductivity	3	1.7296690	0.576556	15,164,365.60	0.0000
Latent heat	3	0.0000060	0.000002	52.59	0.0043
Error	3	0.0000001	0.000000		
Total	15	1.7299981			

significantly different levels of influence on battery temperature reduction.

Among the investigated parameters, thermal conductivity was identified as the dominant factor, exhibiting the highest contribution ratio under all operating conditions. This behavior indicated that the thermal management performance was primarily governed by heat dissipation capability rather than heat storage capacity. In other words, the ability to rapidly transfer heat away from the battery played a more critical role than merely storing thermal energy within the phase change material.

In contrast, the contribution of latent heat was observed to be relatively low. Although latent heat enhanced the energy storage capacity of the phase change material through phase transition, its effectiveness was strongly limited by the rate of heat transfer. Without sufficient thermal conductivity, the stored energy could not be efficiently utilized to reduce peak battery temperature. This finding suggested that phase change alone was not sufficient unless supported by enhanced heat transfer pathways. The effects of density and specific heat capacity were also found to be secondary compared to thermal conductivity, as these parameters mainly

influence the overall thermal inertia of the system but have a limited impact on battery temperature reduction under constrained heat dissipation conditions.

Furthermore, the influence of operating conditions, including discharge rates of 2C and 3C and ambient temperatures of 30 °C and 35 °C, was examined. Although the absolute temperature levels varied with these conditions, the relative importance of thermophysical properties remained largely consistent. This consistency indicated that the dominance of thermal conductivity was robust within the investigated high-power transient operating range.

Unlike several previous studies [60, 61] that emphasized the dominant role of latent heat or phase change temperature, the present results indicated that thermal conductivity was the governing parameter under the investigated conditions. This difference could be attributed to variations in battery type, phase change material composition, parameter ranges, and operating conditions. Therefore, the relative importance of thermophysical parameters was strongly dependent on the material structure. Consequently, the relative importance of thermophysical parameters is strongly dependent on both material structure and operating conditions. The conclusions of this study are valid within the investigated parameter ranges, and different dominance trends may emerge under alternative system configuration parameters such as lower thermal conductivity materials, wider phase change temperature ranges, or lower discharge rates.

Limitations

It should be noted that in the present numerical model, the thermal contact resistance at the battery–PCM interface was neglected, and a perfect thermal contact condition was assumed. This simplification was introduced to reduce model complexity and computational cost. However, in practical battery thermal management systems, the presence of interfacial imperfections, air gaps, and surface roughness—especially in composite phase change materials enhanced with expanded graphite—can introduce non-negligible thermal contact resistance. This effect may increase the overall thermal resistance and reduce the effective heat transfer between the battery and the PCM. Therefore, the current model may slightly underestimate the maximum battery temperature and overestimate the cooling performance of the PCM system. Future work should incorporate interfacial thermal resistance or experimentally calibrated contact conductance values to further improve the accuracy and real-world applicability of the simulations.

Conclusions

A phase change material-based thermal management system was designed for a prismatic lithium iron phosphate battery in this study. Composite phase change materials were prepared by incorporating different concentrations of expanded graphite to enhance the thermophysical characteristics, including density, specific heat capacity, thermal conductivity, and latent heat. The main contribution of this study is the establishment of a quantitative and statistically validated ranking of thermophysical parameters, addressing a key gap in the literature where previous studies have largely relied on qualitative assessments. The principal conclusions are presented below:

- The composite phase change material should have high density, low specific heat capacity, high thermal conductivity, and moderate latent heat to lower the temperature of the lithium-ion battery.
- For all conditions implemented (30 ℃ and 35 ℃ ambient temperatures and 2C-rate and 3C-rate discharge ratios), the thermal conductivity of the composite phase change material was the most influential thermophysical property to decrease the temperature of the lithium-ion battery.
- The impact of the latent heat on lowering the temperature of the lithium-ion battery was lower than that of the other thermophysical properties.
- The contribution of the thermal conductivity was the highest for lowering the temperature of the lithium-ion battery, and its highest value of 97.91% was obtained for the battery discharged at 35 ℃ and 3C-rate.
- The contribution of the latent heat for lowering the temperature of the lithium-ion battery was negligible since its value was lower than 1% for all applied conditions.
- The heat transfer in composite phase change material systems was primarily governed by conduction rather than latent heat storage.

It should be noted that the conclusions are valid within the investigated parameter ranges and operating conditions, and different dominance trends may emerge under alternative system configurations. Overall, the results provide practical guidance for the design of phase change material-based battery thermal management systems, emphasizing the critical importance of enhancing thermal conductivity to achieve effective thermal control.

Author contributions Uğur Moralı was involved in conceptualization, methodology, investigation, visualization, writing—original draft, validation, and software.

Funding Open access funding provided by the Scientific and Technological Research Council of Türkiye (TÜBİTAK). Not applicable.

Data availability No datasets were generated or analyzed during the current study.

Declarations

Conflict of interest The authors declare no conflict of interests.

Ethical approval Not applicable.

Open Access This article is licensed under a Creative Commons Attribution 4.0 International License, which permits use, sharing, adaptation, distribution and reproduction in any medium or format, as long as you give appropriate credit to the original author(s) and the source, provide a link to the Creative Commons licence, and indicate if changes were made. The images or other third party material in this article are included in the article's Creative Commons licence, unless indicated otherwise in a credit line to the material. If material is not included in the article's Creative Commons licence and your intended use is not permitted by statutory regulation or exceeds the permitted use, you will need to obtain permission directly from the copyright holder. To view a copy of this licence, visit http://creativecommons.org/licenses/by/4.0/.

References

1. El Yassini H, Oufaska K, El Maakoul A, Saadeddine S, Yassini KE, Bannari R. Thermal transfer numerical analysis of lithium-ion battery with air-forced and direct liquid cooling. J Therm Anal Calorim. 2025;150:1–30.
2. Farahani SD, Jovini A, Becheikh N, Zekri H, Kolsi L, Karimipour A. A hybrid thermal management approach for lithium-ion batteries using PCM, foam gradient, and GMDH neural networks. Int Commun Heat Mass Transfer. 2025;169:109615.
3. Bamdezh M, Molaeimanesh G, Kand RMS, Mostajeran M. Effects of temperate, cold, and warm climate conditions on electric vehicle and battery thermal management system performance: energy usage, battery aging, and carbon footprints. Energy Convers Manage. 2025;339:119935.
4. Mandlik VT, Sonawane S, Harne M. Numerical analysis and experimental validation of a real-time thermal management and alert system for lithium–ion batteries in electric vehicles. J Therm Anal Calorim. 2025;151:1–13.
5. Sheng L, Wang H, Zhang C, Zhang X. Experimental study on immersion cooling performance of a lithium-ion battery module for commercial/industrial energy storage at different ambient temperatures. Int J Therm Sci. 2026;221:110473.
6. Lei S, Huaiyu L, Bojun T, Chunfeng Z, Xiaojun Z, Liyang W. Experiments on liquid-immersed thermal runaway management for large energy-stored lithium-ion battery modules. Therm Sci Eng Prog. 2025;68:104347.
7. Sheng L, Fu L, Su L, Shen H, Zhang Z. Method to characterize thermal performances of an aluminum-air battery. Energy. 2024;301:131757.
8. Paul D, Nandi A, Bhattacharyya S, Das S, Biswas N. A comprehensive review on lithium-ion battery thermal management (BTM) using phase change materials: advances, challenges, and future perspectives. J Therm Anal Calorim. 2025;150:1–54.
9. Wu Z, Chen H, Jiang L, Zhang P, Ji Z, Luo D. Thermal management of lithium-ion batteries using a PCM-HP-TEC hybrid BTMS: a numerical study. Int Commun Heat Mass Transfer. 2025;169:109702.
10. Sheng L, Lan H, Tao B, Zhang Z, Wang H. Anisotropic thermal conductivity quantification in prismatic lithium-ion batteries. J Energy Storage. 2026;162:122112.
11. Sheng L, Zhang C, Xu J, Zhou Q, Zhang X. Quantitative measurement of thermal performance of a cylindrical lithium-ion battery. Measurement. 2025;239:115458.
12. Sheng L, Zhang C, Xu J, Zhang X, Wang X, Zhang Z. In-situ characterization approach for heat-generating performances of a pouch lithium-ion battery. Appl Therm Eng. 2024;256:124081.
13. Togun H, Basem A, Abdulrazzaq T, Biswas N, Abed AM, Chattopadhyay A, et al. Development and comparative analysis between battery electric vehicles (BEV) and fuel cell electric vehicles (FCEV). Appl Energy. 2025;388:125726.
14. Sheng L, Zhang C, Wang L, Zhou Q, Zhang Z, Zhang X, et al. Experimental-numerical studies on thermal conductivity anisotropy of lithium-ion batteries. J Energy Storage. 2024;103:114139.
15. Wang F, Liu R, Ma X, Zhang Y, Bai G, Ma B, et al. Lithium-ion battery equivalent thermal conductivity testing method based on Bayesian optimization algorithm. J Therm Anal Calorim. 2024;149(24):15073–83.
16. Tang J, Lin X, Mu H, Zhang H, Zhou H, Ma B, et al. Suppression of lithium-ion battery thermal runaway propagation by silica aerogel sheets with different aerogel gel contents and thicknesses. J Therm Anal Calorim. 2025;150:1–13.
17. Nachimuthu S, Alsaif F, Devarajan G, Vairavasundaram I. Real time SOC estimation for Li-ion batteries in electric vehicles using UKBF with online parameter identification. Sci Rep. 2025;15(1):1714.
18. Chaudhari J, Singh GK, Rathod MK, Ali HM. Experimental and computational analysis on lithium-ion battery thermal management system utilizing air cooling with radial fins. J Therm Anal Calorim. 2024;149(1):203–18.
19. Sun W, Li P, Cheng W, Li C, Qi X, Shen H, et al. Novel hybrid thermal management system for cylindrical lithium-ion battery based on CPCM and topology-optimized liquid cooling. Energy. 2025;329:136719.
20. Zhang Q, Xi W, Zhang H, Zhang X. Experimental study of a liquid-vapor phase change cooling method for lithium-ion battery. J Energy Storage. 2025;111:115436.
21. Togun H, Basem A, Jweeg MJ, Kadhum AAH, Mohammed HI, Slimi K, et al. Sustainable cooling solutions for lithium-ion battery thermal management. J Therm Anal Calorim. 2025;150:1–47.
22. Wang C, Wang Y, Zheng Y, Shen K, Lai X, Xu C, et al. Multi-condition simulation and thermal management enhancement of a rectangular-case lithium-ion battery module single-phase immersion cooling system. Int J Therm Sci. 2026;221:110467.
23. Gupta R, Bahga SS, Gupta A. Thermo-electrochemical performance of lithium-ion cells with immersion cooling under various operating conditions. J Energy Storage. 2025;111:115400.
24. Liu Z, Huadan C, Wang B, Li P. Coupling optimization of protruding fin and PCM in hybrid cooling system and cycle strategy matching for lithium-ion battery thermal management. Int J Therm Sci. 2025;207:109372.
25. Wu G, Wu H, Huang B, Zhu W. Hybrid thermal management system of lithium-ion batteries combing phase change material with liquid cooling under high-rate operation. Int J Therm Sci. 2025;218:110117.
26. Chavan S, Venkateswarlu B, Liu J, Joo SW, Kim SC. Investigating the impact of fluid flow channels and cooling fluids on thermal management of lithium-ion battery: a simulation study. J Therm Anal Calorim. 2024;149(4):1629–48.
27. Napa N, Agrawal MK, Tamma B. Impact of active and passive thermal management strategies on the ageing of lithium-ion

battery module under constant and monthly average ambient temperature. J Energy Storage. 2025;113:115642.
28. El Malki A, Ati M, Asch M, Franco AA. A machine learning tool to investigate lithium-ion battery degradation under real automotive conditions. J Power Sources. 2025;630:236048.
29. Kumar K, Sarkar J, Mondal SS. Energy, exergy, and economic evaluations of various cylindrical lithium-ion battery thermal management systems. Int Commun Heat Mass Transfer. 2025;165:109007.
30. Lei S, Bojun T, Huaiyu L, Chunfeng Z, Xiaojun Z. Static method of liquid-immersed thermal regulation for a household energy-storing with lithium-ion batteries. Energy Build. 2025;347:116325.
31. Li K, Guo J, Wu T, Zhang Y, Li C, Zhou H, et al. Development of phase change material for thermal management of lithium-ion batteries: a review. J Therm Anal Calorim. 2025;150:1–26.
32. Mu M, Wu C, Li Y, Chang L, Zhao X, Li M, et al. Research on battery thermal management system of electric mining truck based on topology optimization and PCM coupling. Int Commun Heat Mass Transfer. 2026;171:110122.
33. Koundal S, Sharma SL, Debbarma A. Battery thermal management systems for electric vehicles: an overview of cooling techniques and performance optimization. J Therm Anal Calorim. 2025;150:1–28.
34. Khalaf FA, Tarish AL. Recent update progress for the battery thermal management of electric vehicles: challenges and solutions. J Therm Anal Calorim. 2025;150(16):12135–56.
35. Yang H, Liu N, Gu M, Gao Q, Jiao Z. Multi-objective parameter optimization of U-type air-cooled thermal management system based on a surrogate model. Int J Therm Sci. 2025;212:109707.
36. Kaewchoothong N, Gonsrang S. Enhancing air-cooled battery thermal management using spiral jet arrays in wavy-walled rectangular channels: a numerical study. Int J Therm Sci. 2026;220:110365.
37. Chen X, Yan S, Wang D, Han J, Guan Z, Yin Y, et al. A novel bionic lotus leaf channel liquid cooling plate for enhanced thermal management of lithium-ion batteries. Int J Heat Mass Transfer. 2025;236:126246.
38. Zhao J, Liu H, Zhu J, Ding A, Niu D, Gao H, et al. Numerical investigations of liquid-based battery thermal management performance with distributary manifold channels. Int Commun Heat Mass Transfer. 2025;169:109953.
39. Belwadi ZA, Akula R. Design of a PCM-based thermal management system for cylindrical Li-ion battery using topology optimization. Appl Therm Eng. 2025;270:126143.
40. Alma'asfa SI, Abdul Aziz MS, Khor C, Fraige FY. Thermal management of cylindrical lithium-ion batteries with different fin configurations and phase change material: a numerical analysis. J Therm Anal Calorim. 2025;150(16):12643–62.
41. Xiang X, Yang R, Tehrani NA, Sun H. Advanced topology design of cold plate for battery operating under dynamic conditions. Int J Heat Mass Transfer. 2026;256:128054.
42. Sen S, Mahdi JM, Talebizadehsardari P, La Rocca A, Cairns A. Enhanced thermal management of lithium-ion pouch cells via hybrid approach of phase change material-liquid cooling. Int Commun Heat Mass Transf. 2025;165:108997.
43. Zi J, Long W, Lin T, Zhao R. Optimization and performance analysis of a battery thermal management system combining piped liquid cooling and phase change material. Int J Therm Sci. 2026;220:110401.
44. Heo S, Yook S-J. Development of sodium acetate trihydrate-based composite phase change materials with expanded graphite for nonflammable thermal stabilization and isothermal performance in battery modules. Appl Therm Eng. 2025;271:126353.
45. Kong L, Zheng J, Li Q, Li Y, Kou G, Wen X, et al. Thermal performance of thermal management system combining bionic fern-vein liquid channel with phase change materials for prismatic lithium-ion battery. Int J Therm Sci. 2025;214:109844.
46. Balasubramanian D, Venugopal IP, Subramanian M, Raja V, Kale U, Matijoˇsius J. Study on the battery thermal management system for cylindrical lithium-ion battery with nano-doped phase change material and liquid cooling. Sci Rep. 2025;15(1):24053.
47. Li J, Yang J, Sun Y, Ren X. Performance analysis of battery thermal management system composed of copper foam/paraffin and wavy liquid cooling microchannels. Renew Energy. 2025;256:123928.
48. Kim SW, Son HW, Kim DR. Enhanced cooling effect of core-shell phase change composite thin film on lithium-ion battery for delaying degradation. Int Commun Heat Mass Transf. 2025;169:109530.
49. Lokhande IK, Tiwari N. Experimental and numerical investigation of phase change material filled mini cavity cooling for thermal management of high capacity lithium ion pouch cell. J Power Sources. 2026;661:238553.
50. Rana S, Kumar R, Bharj RS. Experimental and numerical investigation on the thermal performance of fin-enhanced PCM-based temperature regulation system for lithium-ion batteries. Int J Therm Sci. 2026;220:110311.
51. Ji J, An Y, Gu J, Zhang X, Zhang C, Shao Z. Flexible composite phase change materials with high thermal conductivity and electrical insulation properties for lithium-ion battery thermal management. Appl Therm Eng. 2025;266:125706.
52. Nasinathan R, Rajaram K. Measurement of thermal properties and passive cooling of lithium-ion batteries using h-BNNSs and MXene based composite phase change material. J Energy Storage. 2025;132:117809.
53. Subramanian M, Solomon JM, Raja V, Arputharaj BS, Shaik S, Saleel CA, et al. Experimental studies and comprehensive computational investigations on composites-based phase change material for battery thermal management systems in electric vehicles. J Energy Storage. 2024;82:110471.
54. Peng P, Wang Y, Jiang F. Numerical study of PCM thermal behavior of a novel PCM-heat pipe combined system for Li-ion battery thermal management. Appl Therm Eng. 2022;209:118293.
55. Xiang X, Routsi AM, Nagarajan R, Wang Q, Yang R, Esfahani IC, et al. Numerical and experimental investigation of a hybrid battery thermal management system for high-rate applications. J Energy Storage. 2026;141:119081.
56. Saudi MK, Emam M, Hassan H, Sekiguchi H, Khalil AS. Enhancing thermal management of lithium-ion batteries using phase change materials and expanded graphite: an experimental study. J Energy Storage. 2025;130:117427.
57. Jia Y, Liu S, Zhao D, Luo Y, Wang J. Thermal management system with phase change material and liquid cooling for high temperature environments: heat dissipation performance analysis. J Energy Storage. 2026;141:119224.
58. Li H, Wang M, Guo H, Bingwa N, Li G, Xiao Q. Enhancement of thermal management performance in lithium-ion batteries using biomass-derived carbon-enhanced phase change materials. J Energy Storage. 2026;145:119872.
59. Huang R, Li Z, Hong W, Wu Q, Yu X. Experimental and numerical study of PCM thermophysical parameters on lithium-ion battery thermal management. Energy Rep. 2020;6:8–19.
60. Li C, Ding Y, Zhou Z, Jin Y, Ren X, Cao C, et al. Parameter optimization and sensitivity analysis of a lithium-ion battery thermal management system integrated with composite phase change material. Appl Therm Eng. 2023;228:120530.
61. Napa N, Agrawal MK, Tamma B. Phase change material properties identification for the design of efficient thermal management

system for cylindrical lithium-ion battery module. J Energy Storage. 2024;99:113241.
62. Zhang B, Zeng Z, Yuan N, Shi H. Numerical investigation of lithium-ion battery thermal management system performance influenced by physical properties of PCM. J Energy Storage. 2025;117:116141.
63. Zhang Y, Liu H, Liu S, Pan S, Tian C, Hu J. Prediction model of thermal behavior of lithium battery module under high charge-discharge rate. J Energy Storage. 2023;74:109366.
64. Panchal S, Dincer I, Agelin-Chaab M, Fraser R, Fowler M. Experimental and simulated temperature variations in a $LiFePO_4$-20 Ah battery during discharge process. Appl Energy. 2016;180:504–15.
65. Mevawalla A, Shabeer Y, Tran MK, Panchal S, Fowler M, Fraser R. Thermal modelling utilizing multiple experimentally measurable parameters. Batteries. 2022;8(10):147.
66. Zuo W, Zhang Y, Jiaqiang E, Li J, Li Q, Zhang G. Performance comparison between single S-channel and double S-channel cold plate for thermal management of a prismatic $LiFePO_4$ battery. Renew Energy. 2022;192:46–57.
67. Jiang G, Huang J, Fu Y, Cao M, Liu M. Thermal optimization of composite phase change material/expanded graphite for Li-ion battery thermal management. Appl Therm Eng. 2016;108:1119–25.
68. Bodzenta J, Mazur J, Ka´zmierczak-Ba lata A. Thermal properties of compressed expanded graphite: photothermal measurements. Appl Phys B. 2011;105(3):623–30.

Publisher's Note Springer Nature remains neutral with regard to jurisdictional claims in published maps and institutional affiliations.